



# Severe fever with thrombocytopenia syndrome virus (SFTSV)-host interactome screen identifies viral nucleoprotein-associated host factors as potential antiviral targets



Jianli Cao<sup>a,1</sup>, Gang Lu<sup>b,c,d,e,1</sup>, Lei Wen<sup>a</sup>, Peng Luo<sup>a</sup>, Yaoqiang Huang<sup>a</sup>, Ronghui Liang<sup>a</sup>, Kaiming Tang<sup>a</sup>, Zhenzhi Qin<sup>a</sup>, Chris Chun-Yiu Chan<sup>a</sup>, Kenn Ka-Heng Chik<sup>a</sup>, Jiang Du<sup>b,c,d,e</sup>, Feifei Yin<sup>b,c,d,e</sup>, Zi-Wei Ye<sup>a</sup>, Hin Chu<sup>a</sup>, Dong-Yan Jin<sup>f</sup>, Kwok-Yung Yuen<sup>a,c,d,g</sup>, Jasper Fuk-Woo Chan<sup>a,c,d,g,\*</sup>, Shuofeng Yuan<sup>a,\*</sup>

<sup>a</sup> State Key Laboratory of Emerging Infectious Diseases, Carol Yu Centre for Infection, Department of Microbiology, Li Ka Shing Faculty of Medicine, The University of Hong Kong, Pokfulam, Hong Kong Special Administrative Region, China

<sup>b</sup> Key Laboratory of Tropical Translational Medicine of Ministry of Education, Hainan Medical University, Haikou, Hainan 571199, China

<sup>c</sup> Academician Workstation of Hainan Province, Hainan Medical University, Haikou, Hainan 571199, China

<sup>d</sup> Hainan Medical University-The University of Hong Kong Joint Laboratory of Tropical Infectious Diseases, The University of Hong Kong, Pokfulam, Hong Kong Special Administrative Region, China

<sup>e</sup> Department of Pathogen Biology, Hainan Medical University, Haikou, Hainan 571199, China

<sup>f</sup> School of Biomedical Sciences, Li Ka Shing Faculty of Medicine, The University of Hong Kong, Pokfulam, Hong Kong Special Administrative Region, China

<sup>g</sup> Department of Clinical Microbiology and Infection Control, The University of Hong Kong-Shenzhen Hospital, Shenzhen, China

## ARTICLE INFO

### Article history:

Received 6 July 2021

Received in revised form 29 September 2021

Accepted 29 September 2021

Available online 01 October 2021

### Keywords:

Artemimol  
Bunyavirales  
Interactome  
Omacetaxine mepesuccinate  
Pathogenesis  
SFTSV  
Treatment

## ABSTRACT

Severe fever with thrombocytopenia syndrome virus (SFTSV) is an emerging tick-borne virus that causes severe infection in humans characterized by an acute febrile illness with thrombocytopenia and hemorrhagic complications, and a mortality rate of up to 30%. Understanding on virus-host protein interactions may facilitate the identification of druggable antiviral targets. Herein, we utilized liquid chromatography-tandem mass spectrometry to characterize the SFTSV interactome in human embryonic kidney-derived permanent culture (HEK-293T) cells. We identified 445 host proteins that co-precipitated with the viral glycoprotein N, glycoprotein C, nucleoprotein, or nonstructural protein. A network of SFTSV-host protein interactions based on reduced viral fitness affected upon host factor down-regulation was then generated. Screening of the DrugBank database revealed numerous drug compounds that inhibited the prioritized host factors in this SFTSV interactome. Among these drug compounds, the clinically approved artemimol (an antimalarial) and omacetaxine mepesuccinate (a cephalotaxine) were found to exhibit anti-SFTSV activity *in vitro*. The higher selectivity of artemimol (71.83) than omacetaxine mepesuccinate (8.00) highlights artemimol's potential for further antiviral development. Mechanistic evaluation showed that artemimol interfered with the interaction between the SFTSV nucleoprotein and the host glucose-6-phosphate isomerase (GPI), and that omacetaxine mepesuccinate interfered with the interaction between the viral nucleoprotein with the host ribosomal protein L3 (RPL3). In summary, the novel interactomic data in this study revealed the virus-host protein interactions in SFTSV infection and facilitated the discovery of potential anti-SFTSV treatments.

© 2021 The Author(s). Published by Elsevier B.V. on behalf of Research Network of Computational and Structural Biotechnology. This is an open access article under the CC BY-NC-ND license (<http://creativecommons.org/licenses/by-nc-nd/4.0/>).

\* Corresponding authors at: Department of Clinical Microbiology and Infection Control, The University of Hong Kong-Shenzhen Hospital, Shenzhen, China; and State Key Laboratory of Emerging Infectious Diseases, Carol Yu Centre for Infection, Department of Microbiology, Li Ka Shing Faculty of Medicine, The University of Hong Kong, Pokfulam, Hong Kong Special Administrative Region, China (J. F.-W. Chan and S. Yuan).

E-mail addresses: [jfwchan@hku.hk](mailto:jfwchan@hku.hk) (J.F.-W. Chan), [yuansf@hku.hk](mailto:yuansf@hku.hk) (S. Yuan).

<sup>1</sup> Co-first authors.

## 1. Introduction

Severe fever with thrombocytopenia syndrome virus (SFTSV) is an emerging tick-borne virus that can cause severe infection in human. Since the discovery of SFTSV in Henan, China, the virus has also been isolated from infected humans, ticks, and/or mammals in Japan, South Korea, and Vietnam [1–5]. SFTS is characterized by acute fever, thrombocytopenia, and hemorrhagic

complications. Other systemic manifestations such as hepatosplenomegaly, lymphadenopathy, gastrointestinal upset, slurred speech, and coma may also occur [1,6]. The mortality rate of SFTS may be as high as 17%–30% [1,6]. Despite the severe clinical manifestations and high mortality rate of SFTS, comprehensive understanding on the pathogenesis and effective antivirals are lacking.

Like other viruses, SFTSV hijacks the host cell machinery to facilitate its own replication. A comprehensive investigation of the virus-host protein interactions in SFTSV infection would improve our understanding of the virus replication cycle and identify potential antiviral targets. SFTSV is an enveloped, single-stranded, negative-sense RNA virus belonging to the genus *Banyangvirus*, family *Phenuiviridae*, order *Bunyavirales*. The genome of SFTSV consists of three RNA segments, namely, the large (L), medium (M), and small (S) segments. The L segment encodes the RNA-dependent RNA polymerase (RdRp), which mediates viral RNA replication and synthesis. The M segment encodes the viral envelope glycoproteins, glycoprotein N (Gn) and glycoprotein C (Gc), which mediate fusion between the viral and host cell membranes. The S segment encodes the viral nucleoprotein (NP) and the nonstructural protein (NSs) [7]. NP is the most abundantly expressed protein in SFTSV viral particles and infected cells. NSs is a potentially important virulence factor of SFTSV that inhibits the host innate antiviral response.

Host factors required for viral replication are less likely to mutate under drug-mediated selective pressure than viral proteins [8]. A recent study uncovered that the SFTSV NSs interacts with cyclin-dependent kinase (CDK1) to induce G2 cell cycle arrest and positively regulate viral replication [9]. Another recent report identified the role of the SFTSV NSs to interact with TANK-binding kinase 1 (TBK1) and suppress the host interferon response [10]. Importantly, the interactions between the SFTSV NSs and TBK1 could be inhibited by PS-341, the first clinically approved proteasome inhibitor [11]. At present, a comprehensive survey on the SFTSV interactome is lacking. To address this knowledge gap, we conducted a systematic analysis of the SFTSV interactome, followed by *in vitro* validation studies and a systematic assessment of the functional roles of these host proteins in SFTSV replication (Fig. 1). Importantly, this information facilitates the discovery of novel druggable target for anti-SFTSV development.

## 2. Materials and methods

### 2.1. Virus, cell lines, and drug compounds

SFTSV HB29 strain (a gift from Dr. Benjamin Brennan, MRC-University of Glasgow Centre for Virus Research and Professor Mifang Liang, China CDC) was propagated in Vero cells (ATCC® CCL-81™) and kept at  $-80^{\circ}\text{C}$  in aliquots. Plaque forming unit (PFU) assay was performed to titrate the cultured virus as previously described [12]. HEK-293T (human embryonic kidney-derived permanent culture cells, ATCC, CRL-3216) and Huh-7 (human hepatoma cells, JCRB, 0403) cell lines were maintained in Dulbecco's modified eagle medium (DMEM, Gibco, CA, USA) supplemented with 10% heat-inactivated fetal bovine serum (FBS, Gibco), 50 U/ml penicillin, and 50  $\mu\text{g}/\text{ml}$  streptomycin as previously described [12]. All cell lines were confirmed to be free of mycoplasma contamination by Plasmoguard Test (InvivoGen, San Diego, CA, USA) and were morphologically consistent with those provided by the manufactures. Upon virus infection, the cells were maintained in FBS-free medium with or without drug compounds. All experiments involving live SFTSV followed the approved standard operating procedures of the Biosafety Level 3 facility at the Department of Microbiology, The University of Hong Kong [12]. All the

tested drug compounds were purchased from MedChem Express (Monmouth Junction, NJ, USA) unless otherwise specified.

### 2.2. Cell viability assay

The CellTiterGlo® luminescent assay (Promega Corporation, Madison, WI, USA) was performed to detect the cytotoxicity of the selected drug compounds as previously described [13]. Briefly, Huh-7 cells ( $4 \times 10^4$  cells/well) were incubated with different concentrations of the individual drug compounds for 48 h, followed by the addition of substrate and measurement of luminance 10 min later. The 50% cytotoxic concentrations ( $\text{CC}_{50}$ ) of the drug compounds were calculated by Prism7 (GraphPad).

### 2.3. siRNA library screening and validation

The ON-TARGETplus SMARTpool protein kinases siRNA library that targets the mRNAs of 254 genes, was obtained from Dharmacon (Lafayette, CO, USA). Each individual siRNA SMARTpool consists of four siRNAs targeting the same gene. A non-targeting (scrambled) siRNA (Cat no. D-001810-10; Dharmacon) was included as a negative control, and a myosin heavy chain 9 (MYH9) siRNA (Cat no. L-007668-00-0005; Dharmacon) was included as a positive control. Stock solutions (2  $\mu\text{M}$ ) of siRNA SMARTpools were prepared by dissolving 0.1 nmol of an siRNA SMARTpool in 50  $\mu\text{l}$  of  $1 \times$  siRNA buffer (Dharmacon) according to the manufacturer's instructions.

The siRNA screening was performed as we previously described with few modifications [8]. Briefly, Huh-7 cells in 96-well plates containing  $\sim 10^4$  cells per well were transfected with a 100  $\mu\text{l}$  mixture containing 60 nM siRNA, 0.5  $\mu\text{l}$  Lipofectamine RNAiMAX (Thermo Fisher), Opti-MEM (Invitrogen), and antibiotic-free cell culture medium. Transfection complexes were prepared in 96-well plates. At 48 h after second transfection, the medium was replaced and the cells were infected with SFTSV [multiplicity of infection (MOI) = 0.01]. At 48 h after virus infection, the cells were collected into RNA lysis buffer (QIAGEN), followed by total nucleic acid extraction. The viral RNA load was determined by quantitative reverse transcription-polymerase chain reaction (qRT-PCR). The values obtained using scrambled siRNA-transfected cells were set as negative controls. The results of each library screen were summarized and used for further data analysis, including the assignment of gene identifiers to each well. Finally, the data from the two independent library screens were combined and summarized.

### 2.4. Viral load reduction assay

Viral load reduction assay was performed as described previously with modifications [14]. Briefly, Huh-7 cells seeded in 96-well plates were infected with SFTSV for 1 h, followed by phosphate-buffered saline (PBS) wash and replacement with fresh DMEM medium containing various drug compounds at different concentrations or 0.1% DMSO (as the vehicle control). Then, the culture supernatants were collected at 2 dpi, followed by total nucleic acid extraction. qRT-PCR with previously established primers (forward 5'-GGGTCCCTGAAGGAGTTGTTAAA-3' and reverse 5'-TGCCTTACCAAGACTATCAATGT-3') and probe (FITC-TTCTGTCTTGCTGGCTCCGCGC-BHQ) targeting the S segment of the SFTSV genome was then performed using the Roche LightCycler Real-time PCR system. To plot the half maximal effective concentration ( $\text{EC}_{50}$ ) of the drug compounds, the collected supernatants were subjected to standard plaque assay on Huh-7 cells and calculated by Prism7 (GraphPad).

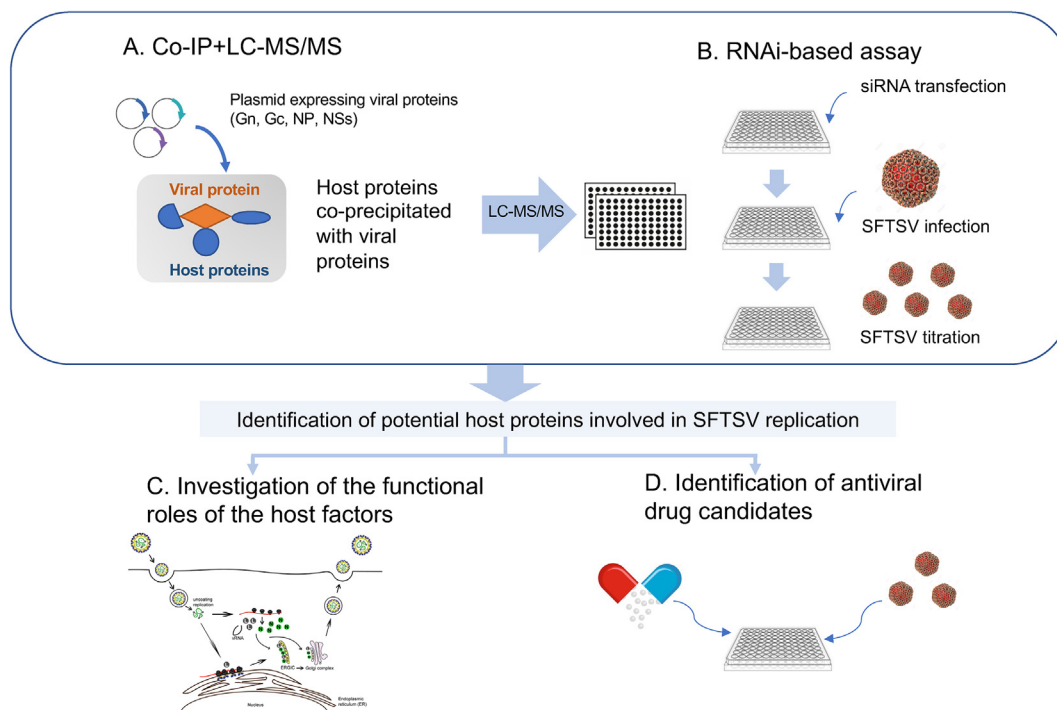


**Fig. 1.** Flowchart of the study. (A) Pulldown of viral proteins and associated proteins, followed by characterization by LC-MS/MS. (B) Functional validation of the enriched protein candidates. Corresponding siRNAs were transfected into Huh7 cells, resulting in RNAi-mediated silencing of the individual target genes. SFTSV infection was performed after gene-silencing, followed by virus titration by qRT-PCR. (C) Identification of the functional role of the selected host factors in SFTSV replication cycle. (D) Antiviral evaluation of the selected drug compounds targeting the SFTSV-host protein–protein interactions. Abbreviations: Co-IP, co-immunoprecipitation; Gc, glycoprotein C; Gn, glycoprotein N; LC-MS/MS, liquid chromatography–tandem mass spectrometry; NP, nucleoprotein; NSs, non-structural protein.

## 2.5. Pull-down assay and mass spectrometry

For the pull-down and co-immunoprecipitation assays with magnetic beads conjugated with anti-HA antibody, lysates of the plasmid-transfected HEK-293T cells were incubated with anti-HA magnetic beads (ChemCruz, sc-500773A) at 4 °C overnight. Following intensive washing, the elution samples were analyzed by mass spectrometry and western-blotting, respectively. For mass spectrometry analysis, the pull-down samples were subjected to in-gel digestion with trypsin, following SDS-PAGE for validation. The digested peptides were analyzed by liquid chromatography–tandem mass spectrometry (LC-MS/MS) using the nano-LC-equipped TripleTOF 5600 system (AB SCIEX). Raw tandem spectra were searched against Unified Protein database (UniProt) with the ProteinPilot Software 5.0 (AB SCIEX). The data selected for further analysis were based on the false discovery rate (FDR) of  $\leq 1\%$  for protein identification.

## 2.6. Western blotting

For Western blotting, total cell lysates were prepared in RIPA Lysis and Extraction Buffer (Thermo Fisher). Then, the samples were heated at 95 °C for 10 min. Following SDS-PAGE, proteins were transferred to PVDF membranes (GE Healthcare) by semidry blotting and the membranes were blocked with 5% nonfat dry milk in PBS containing 0.1% Tween 20 (PBST).

## 2.7. Plasmids and antibodies

The plasmids and antibodies, including GPI Human Tagged ORF Clone (RC230292, Origene), RPL3 Human Tagged ORF Clone (RC217987, Origene), mouse anti-HA (Cat #26183; Thermo Fisher), rabbit anti-Myc (Cat #PA1-981, Thermo Fisher), goat anti-mouse-IgG (H + L) HRP (A16072SAMPLE, Thermo Fisher), and goat anti-

rabbit-IgG (H + L) HRP (A16104SAMPLE, Thermo Fisher) were purchased from commercial sources.

## 2.8. Molecular docking

The crystal structure of GPI was downloaded from the Protein Data Bank (PDB code: 6XUI) [15]. Protonation states of the side chains were predicted using PROPKA3.1 server [16]. The structure of arteminol was retrieved from Drugbank (DB11638) and was prepared with OpenBabel 2.3.1, including 3D conformer search, bond order assignment, hydrogen addition, and partial charge calculation. Molecular docking was performed by using Leadfinder docking with default parameters ([17]). The key residues surrounding arteminol were visualized with PyMol (<https://pymol.org/2/>).

## 2.9. Gene Ontology

Cluster Profiler, an R package for comparing biological themes among gene clusters, was used for the Gene Ontology enrichment in this study [18].

## 2.10. Illustrations

The illustrations in Fig. 2 were created with BioRender software (<https://biorender.com/>).

## 3. Results

### 3.1. Purification and identification of SFTSV proteins

To identify human proteins associated with SFTSV, we cloned the sequence of each SFTSV protein using a mammalian expression vector. Each protein was fused with a HA tag at either its amino (N) or carboxy (C) terminus, including Gn, Gc, NP, and NSs (Fig. 2A).

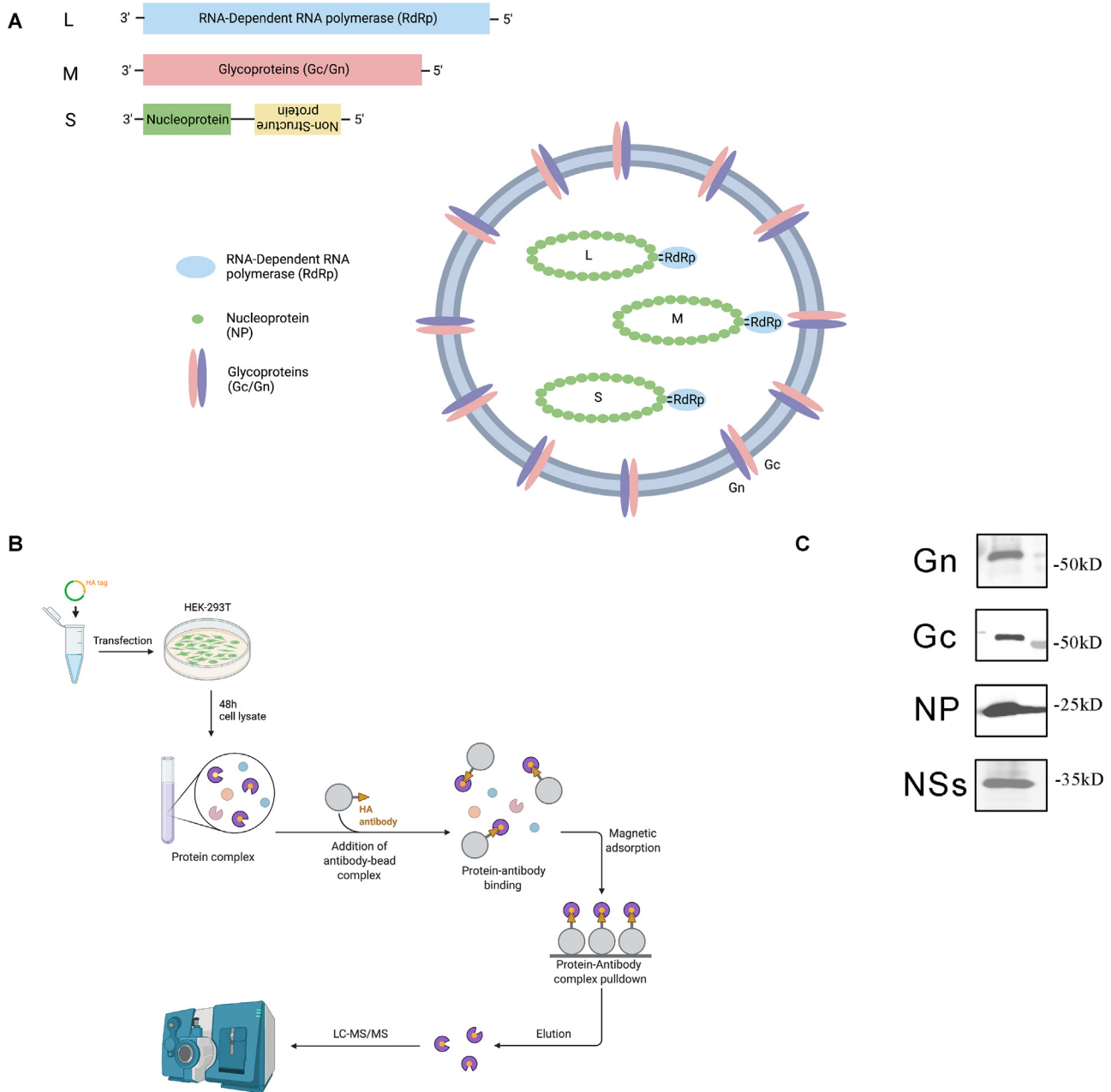


**Fig. 2.** Identification of SFTSV protein-bound host factors. (A) Organization of the SFTSV genome. The tripartite segmented genome is comprised of three segments: Large (L), Medium (M), and Small (S). The L segment encodes the RNA-dependent RNA polymerase. The M segment encodes two glycoproteins Gn and Gc. The S segment encodes the viral nucleoprotein (NP) and non-structural protein (NSs), which is encoded in the opposite orientation to the viral NP. (B) Isolation and analysis of the host-bound viral protein complexes. Briefly, the SFTSV open reading frame plasmids which contains HA-tag were transfected into HEK-293T cells. After incubation for 48 h, the cell lysates were collected and pulled down using HA-tag beads, followed by protein ID by LC-MS/MS. (C) The Western blotting images of each viral protein after pull-down and detection by anti-HA tag antibody.

RdRp was not included due to extraordinarily low expression yield. Empty vectors with independent tags at either terminus were used to minimize the possibility of false-positive protein–protein interactions due to tag masking. The clones were transfected into HEK-293T cells with tagged proteins purified 48 h post-transfection. The final eluates were then analyzed by SDS-PAGE for quality control and by LC-MS/MS to identify interaction partners (Fig. 2B and C).

### 3.2. Analysis of SFTSV-human protein–protein interactions

As a result, mass spectrometry analyses of the co-precipitated proteins identified 445 host proteins in total: 87, 166, 100, and

92 host proteins co-precipitated with the viral Gn, Gc, NP, and NSs proteins, respectively (Fig. 3). Based on the binding partners, we performed pathway enrichment and network plot of individual viral proteins. The key element of virus entry, Gn, is highly “membrane” relevant, suggesting its role during virus-cell membrane fusion (Fig. 4 and Supplementary Fig. 1). The top three biological processes of Gc-associated host factors were mapped to “intermediate filament-based organization or process”, which is a primary component of the cytoskeleton (Fig. 4 and Supplementary Fig. 2). This result indicate an important role of Gc during SFTSV entry and in particular endocytosis. Expectedly, NP-associated host factors are dominantly enriched in RNA processing (Fig. 4 and

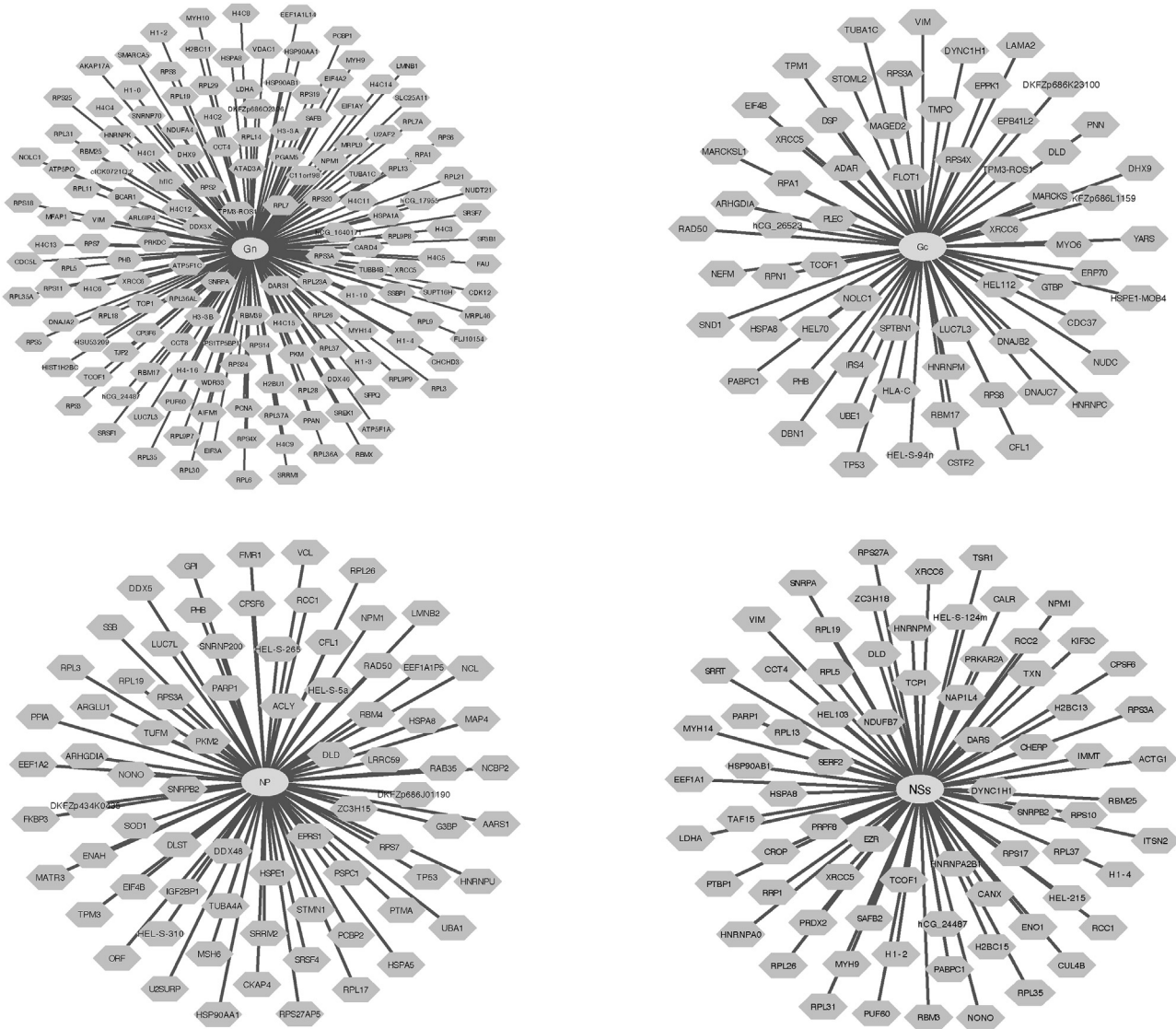


Fig. 3. SFTSV-host protein–protein interaction network illustrating each SFTSV protein and its associated host cellular factors. (For interpretation of the references to color in this figure legend, the reader is referred to the web version of this article.)

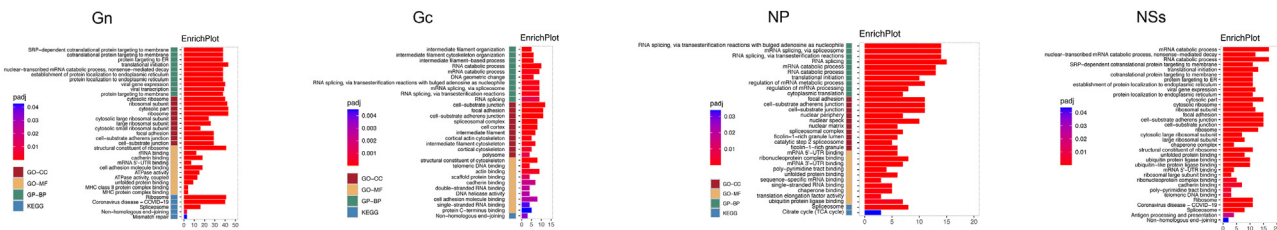


Fig. 4. Gene Ontology enrichment analysis was performed on the identified host cellular factors based on each SFTSV protein. Abbreviations: BP, biological process; CC, cellular components; KEGG, Kyoto encyclopedia of genes and genomes; MF: molecular function.

Supplementary Fig. 3), whereas NSs appears to be a versatile protein that is involved in both viral replication and the translation process (Fig. 4 and Supplementary Fig. 4).

### 3.3. Validation of functional host proteins in the SFTSV interactome

The co-precipitated host proteins may be specific binding partners of SFTSV proteins with essential or non-essential functions in the viral replication cycle. Alternatively, they may be non-specific

or false-positive binding partners resulting from experimental artifacts such as the overexpression of viral proteins in our assay and/or the absence of other viral components. To identify host factors that are specifically involved in SFTSV replication, we transfected SFTSV-permissive Huh7 cells with siRNAs targeted to each of the 254 candidate host genes with top credibility after MS analysis (ie: number of peptide replicates > 2). At 24 h post-siRNA-transfection, the Huh7 cells were infected with SFTSV (MOI = 0.01) and then the culture supernatants were harvested

for virus titration after another 48 h (Fig. 5A). In parallel, we examined the cell viability of siRNA-transfected cells using the CellTiter-Glo® assay to exclude cell death-related SFTSV suppression due to depletion of host genes. As a result, we identified 10 host genes whose knockdown consistently led to reduced SFTSV replication. These genes included 60S ribosomal protein L17 (RPL17), Ubiquitin Like Modifier Activating Enzyme 1 (UBA1), Ribosomal Protein L3 (RPL3), Glucose-6-Phosphate Isomerase (GPI), Peptidylprolyl Isomerase A (PPIA), Ribosomal Protein S3A (RPS3A), Kinesin Family Member 3C (KIF3C), FAU Ubiquitin Like And Ribosomal Protein S30 Fusion (FAU), Nuclear Distribution C, Dynein Complex Regulator (NUDC), and Ezrin (EZR). (Fig. 5B).

### 3.4. Exploration of antiviral targets based on the 10 SFTSV-dependency host factors

To identify potential antiviral targets among the identified host factors, we searched the DrugBank database for drug compounds that suppress these 10 host factors. The DrugBank database contains >9000 entries including 2037 FDA-approved small molecule drug compounds, 241 FDA-approved biotech (protein/peptide) drug compounds, 96 nutraceuticals, and over 7000 experimental drug compounds [19]. We identified 24 drug compounds that were associated with these 10 host factors. Based on their availability, we further selected 6 of these 24 drug compounds for further

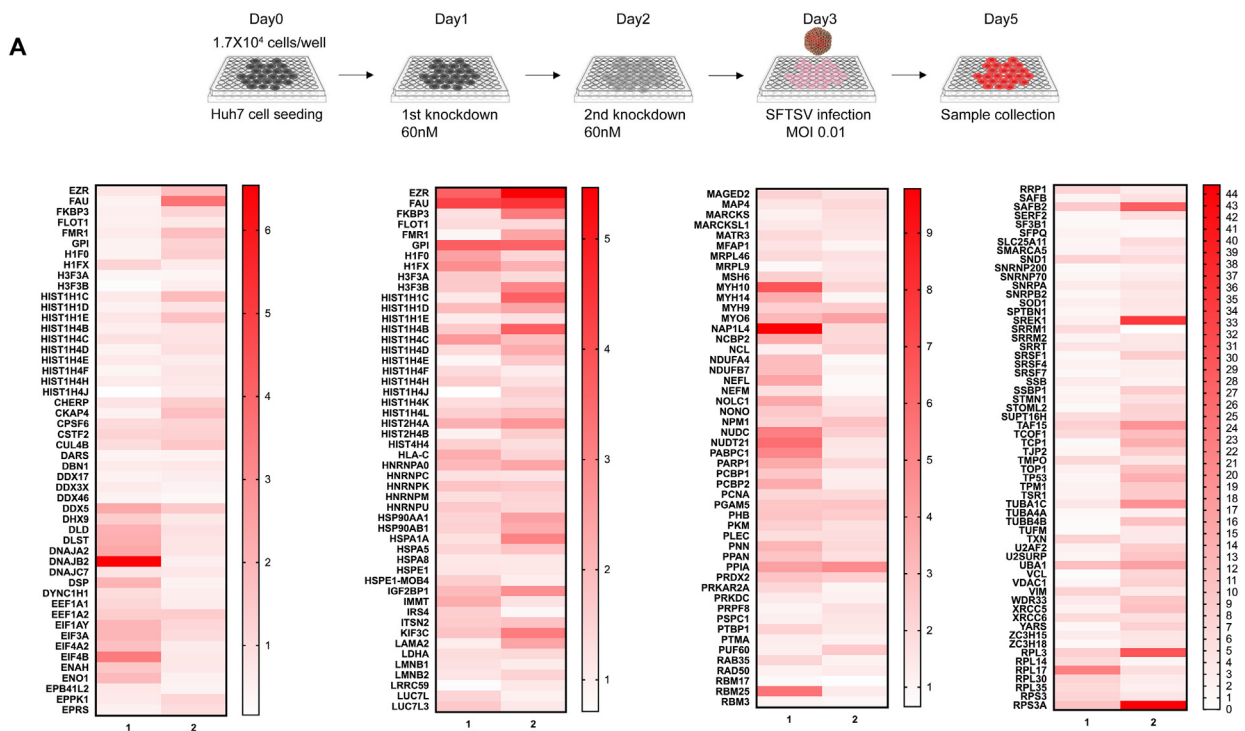


**Fig. 5.** Host small interfering RNA (siRNA) screens to identify host factors that affect SFTSV replication. (A) Upper panel: experimental design of the siRNA library screening. Briefly, Huh7 cells were transfected once daily (60 nM) for two times before SFTSV infection (MOI = 0.01). After another 48 h, cell culture supernatant was harvested for viral load determination. Lower panel: heat map showing SFTSV viral load reduction after individual siRNA knockdown. The results were normalized by the infected cells that were transfected with scrambled siRNA. (B) A list of the host factors whose knockdown reduced SFTSV replication.

antiviral testing. To determine the inhibitory effects on SFTSV replication of these 6 drug compounds, SFTSV-infected Huh7 cells were treated with each drug compound at 1.25  $\mu\text{M}$ , 5.00  $\mu\text{M}$ , and 20.00  $\mu\text{M}$ . During the primary screening, only arteminol, an artemisinin derivative antimalarial agent, showed potent anti-SFTSV activity and in a dose-dependent manner. Omacetaxine mepesuccinate, a natural plant alkaloid derived from *Cephalotaxus fortunei* used in the treatment of chronic myeloid leukemia, showed cellular toxicity at concentrations of  $>1 \mu\text{M}$ . Quercetin (plant flavonol), monastrol (kinesin-5 inhibitor), pevonedistat (NEDD8 inhibitor), and phenethyl isothiocyanate (naturally occurring isothiocyanate) showed either marginal effect or lack of dose-dependent antiviral effect, and were therefore not prioritized for additional characterization (Fig. 6).

### 3.5. Characterization of the antiviral effects of arteminol and omacetaxine mepesuccinate

To characterize the therapeutic potential of arteminol and omacetaxine mepesuccinate, we determined the  $\text{CC}_{50}$  and  $\text{EC}_{50}$  of each drug compound in Huh7 cells. As shown in Fig. 7A, the  $\text{CC}_{50}$  of arteminol and omacetaxine mepesuccinate in Huh7 cells were 17.24  $\mu\text{M}$  and 0.56  $\mu\text{M}$ , respectively. In the viral load reduction assay, the  $\text{EC}_{50}$  of arteminol and omacetaxine mepesuccinate were 0.24  $\mu\text{M}$  and 0.07  $\mu\text{M}$ , respectively. The selectivity index ( $\text{CC}_{50}/\text{EC}_{50}$ ) of arteminol (71.83) was much higher than that of omacetaxine mepesuccinate (8.00), suggesting that arteminol may have higher potential for *in vivo* use.

### 3.6. Mode of action of arteminol and omacetaxine mepesuccinate against SFTSV

We investigated the mode of action of arteminol and omacetaxine mepesuccinate against SFTSV. As indicated in our interactome, arteminol potentially disrupts SFTSV viral NP and human glucose-6-phosphate isomerase (GPI), whereas omacetaxine mepesuccinate targets the interaction between viral NP and host receptor-like protein 3 (RPL3). Co-transfection of GPI/NP plasmids and RPL3/NP plasmids was performed in HEK-293T cells, followed by pull-down of the HA-tagged viral NP complex. Apparently, all three proteins were well expressed in HEK-293T cells (Input,

Fig. 7B). Both GPI and RPL3 proteins were detectable in co-immunoprecipitation groups, indicating direct SFTSV-NP/GPI and SFTSV-NP/RPL3 binding (Co-IP, Fig. 7B). To further validate the linkage between protein–protein dissociation and the observed antiviral effect, we treated HEK-293T cells expressing HA-tagged SFTSV-NP and GPI or RPL3 with different concentrations of arteminol or omacetaxine mepesuccinate. Our results showed that addition of either arteminol or omacetaxine mepesuccinate disrupted that binding between SFTSV-NP and its host counterpart proteins (Fig. 7C). The dose-dependent effect appears to be more evident in the omacetaxine mepesuccinate-treated group than the arteminol-treated group, which is consistent with their antiviral effects (Fig. 7A). Under non-toxic concentrations, complete virus suppression and SFTSV-NP-RPL3 dissociation is achievable with omacetaxine mepesuccinate, but not arteminol. Next, molecular docking analysis was performed to model the protein–drug compound interactions. Because the crystal structure of GPI but not that of RPL3 was available, we focused on the interaction between arteminol and GPI only. Our prediction shows that arteminol contacts GPI via the G158 and E357 amino acid residues, which might also contribute to viral NP/GPI integration (Fig. 7D). Collectively, we demonstrate that drug compounds interfering with the binding between SFTSV NP and host proteins may serve as potential anti-SFTSV treatments.

## 4. Discussion

Viruses are obligatory intracellular microorganisms that utilize the host cell machinery to replicate. Interference with the interactions between the key viral and host proteins involved in viral replication may be potential antiviral treatment strategies. Despite its clinical importance, the virus–host interactions in SFTSV infection remain incompletely understood. Previously, a variety of technologies have been used to study virus–host protein–protein interactions. These include tandem affinity purification coupled with mass spectrometry (TAP-MS), two-hybrid system screens, and protein–fragment complementation assays [20]. In this study, we exploited LC-MS/MS to characterize the interactome in SFTSV infection and utilized these novel interactomic data to identify potential antiviral treatments for this highly lethal emerging viral infection.

We identified 445 host proteins that co-precipitated with the viral Gn, Gc, NP, or NSs proteins in the SFTSV interactome in HEK-293T cells. Our downstream *in silico* and *in vitro* analyses further prioritized 10 host genes that were associated with significantly reduction of SFTSV viral load when being knocked down with gene-specific siRNA. Screening of the DrugBank database led to the discovery of numerous drug compounds that target these 10 host genes. Among these drug compounds, arteminol and omacetaxine mepesuccinate demonstrated the most potent inhibitory effects against SFTSV replication, with arteminol having a much higher selectivity index (71.83) than omacetaxine mepesuccinate (8.00).

Arteminol (also known as dihydroqinghaosu, dihydroartemisinin, or DHA) is the active metabolite of artemisinin compounds such as artemisinin, artesunate, and artemether. In CD-1 male mice that received arteminol (up to 1200 mg/kg), no signs of toxicity was observed, which indicated the drug compound's excellent safety profile. It was first authorized for marketing by the European Medicines Agency in October 2011 in combination with piper-quine as Eurartesim. Like its precursor artemisinin, arteminol is available as an antimalarial. Artemisinin is a natural product derived from the Chinese herb *Artemisia annua* and is one of the most effective antimalarials available [21]. Interestingly, artemisinin was found to exhibit antiviral activities against various DNA

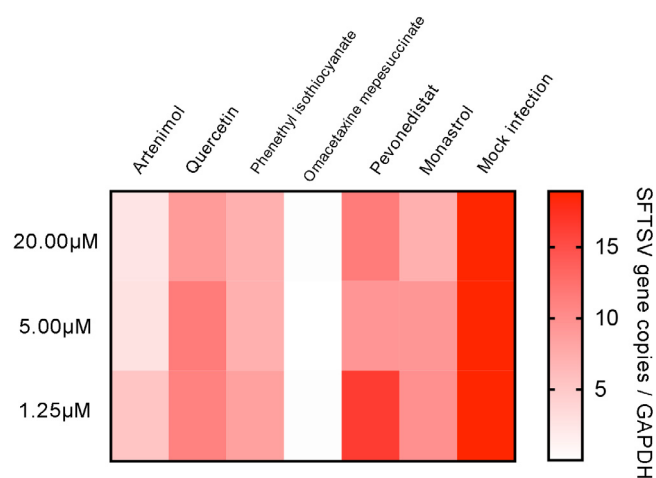


**Fig. 6.** Primary screening of available drug compounds targeting the identified host factors. The heat map of SFTSV viral load after drug compound treatment was shown. Huh-7 cells were infected by SFTSV (MOI = 0.10) and treated by different concentrations of each drug compound as indicated. The viral load in the cell lysate was measured at 48 hpi and normalized by GAPDH.

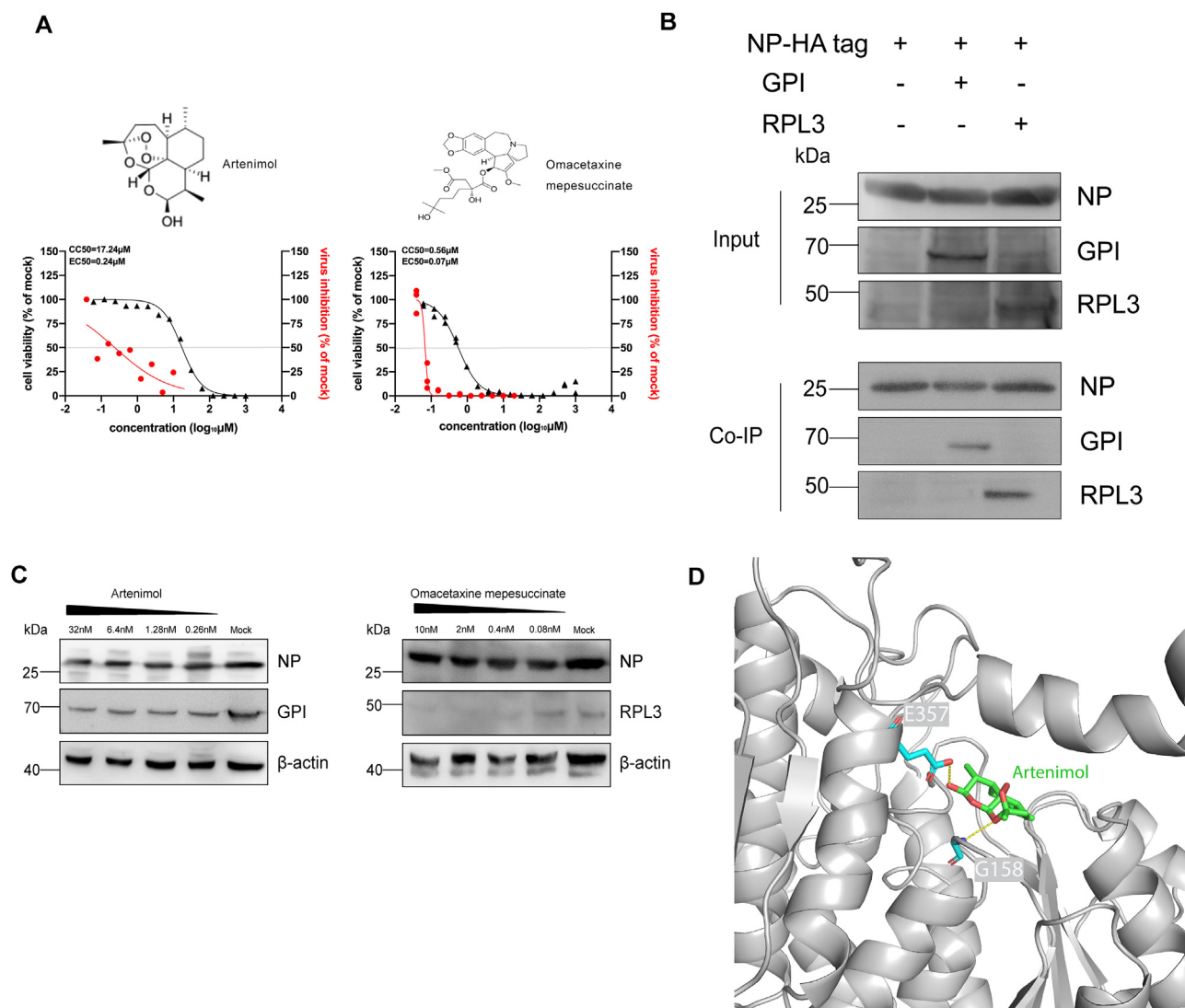


**Fig. 7.** Characterization of the selected SFTSV inhibitors. (A) Dose-response analyses of artemimol and omacetaxine mepesuccinate are shown, depicting both the antiviral activity (red) and cytotoxicity (black). The grey line indicates 50% of the mock-treated control. The  $EC_{50}$ ,  $CC_{50}$ , and chemical structure of each drug compound are shown. (B) Co-immunoprecipitation assay was conducted in HEK-293T cell transfected with SFTSV nucleoprotein together with either GPI or RPL3 plasmids. After pull-down, the viral nucleoprotein was detected by anti-HA antibody, while GPI and RPL3 were detected by anti-Myc antibodies. (C) Co-immunoprecipitation assay with the treatment of artemimol or omacetaxine mepesuccinate at the indicated concentrations. (D) Molecular docking analysis predicted the interface between artemimol and GPI. The protein is shown as grey ribbons and the drug compound as color sticks. (For interpretation of the references to color in this figure legend, the reader is referred to the web version of this article.)

viruses, including members of the *Herpesviridae* (herpes simplex viruses 1 and 2, Epstein-Barr virus, human cytomegalovirus, and human herpesvirus 6) and *Hepadnaviridae* (hepatitis B virus) families [22]. Our findings expand the antiviral spectrum of artemisinin compounds to SFTSV and highlight the need to further characterize these drug compounds' full antiviral spectrum against other related RNA viruses.

Omacetaxine mepesuccinate, also known as homoharringtonine, is a clinically available cephalotaxine indicated for the treatment of chronic myeloid leukemia in patients with refractory disease or intolerance to tyrosine kinase inhibitors (trade name: Synribo) [23]. Importantly, a single dose of omacetaxine mepesuccinate can achieve a peak serum concentration ( $C_{max}$ ) of up to 56.0 ng/ml (equivalent to about 102 nM), which is above its  $EC_{50}$  against SFTSV. Further drug compound optimization of omacetaxine mepesuccinate to reduce its cellular toxicity and to minimize its side effect of cytopenia may increase its potential for clinical use in SFTSV infection.

Mechanistically, our interactome predicted that artemimol likely interfered with the binding between the SFTSV NP and the host GPI. The SFTSV NP encoded by the S segment is the main structural component of the viral ribonucleoprotein (RNP) and plays an important role in viral RNA replication, transcription, and synthesis [24]. Polymerized NP coats viral RNA to assemble the integrity of RNP. Multiple copies of the SFTSV NP are polymerized and then encapsidate a viral RNA segment that associate with one copy of the viral RdRp to form the RNP. RNPs act as the RNA synthesis machinery in the host cell cytoplasm and can also be packaged by the viral membrane as the structural core of the generated virions [25]. Structural studies showed that the viral NP is composed of a core domain that is divided into an N-lobe and a C-lobe, and an N-terminal arm (N-arm) [26]. The N-terminal arm mediates NP polymerization by binding to the lateral N promoter to facilitate encapsidation of the viral RNA and assembly of the RNP [27]. Considering the central roles of the viral NP and the assembled RNP in virus replication and proliferation, these funda-



mental viral elements may be targeted by the host immune system to restrict virus replication. Importantly, the amino acid sequences of the NP of SFTSV and related bunyaviruses share highly similarity [1,28,29]. Thus, antiviral strategies that target the viral NP may represent broad-spectrum treatment options for a wide range of bunyaviruses.

In summary, our interactomic findings characterized the virus-host protein interactions in SFTSV infection and facilitated the identification of clinically available drug compounds that target the binding between SFTSV-NP and the host GPI or RPL3 as potential antiviral treatment options for this emerging viral infection. Further evaluations of these drug compounds in suitable animal models should be considered.

## Funding

This study was partly supported by funding from the Health and Medical Research Fund (CID-HKU1-10 and 19180502), the Food and Health Bureau, The Government of the Hong Kong Special Administrative Region; the Consultancy Service for Enhancing Laboratory Surveillance of Emerging Infectious Diseases and Research Capability on Antimicrobial Resistance for Department of Health of the Hong Kong Special Administrative Region Government; Innovation and Technology Fund (ITF), the Government of the Hong Kong Special Administrative Region; Sanming Project of Medicine in Shenzhen, China (SZSM201911014); the High Level-Hospital Program, Health Commission of Guangdong Province, China; the Major Science and Technology Program of Hainan Province (ZDKJ202003); the research project of Hainan academician innovation platform (YSPTZX202004); and the Hainan talent development project (SRC200003); and donations of Lee Wan Keung Charity Foundation Limited, Richard Yu and Carol Yu, Shaw Foundation Hong Kong, Michael Seak-Kan Tong, Hui Ming, Hui Hoy and Chow Sin Lan Charity Fund Limited, Chan Yin Chuen Memorial Charitable Foundation, Marina Man-Wai Lee, the Hong Kong Hainan Commercial Association South China Microbiology Research Fund, and Lo Ying Shek Chi Wai Foundation. The funding sources had no role in the study design, data collection, analysis, interpretation, or writing of the report.

## CRedit authorship contribution statement

**Jianli Cao:** Formal analysis, Investigation, Writing - original draft. **Gang Lu:** Formal analysis, Funding acquisition, Writing - review & editing. **Lei Wen:** Formal analysis, Investigation, Methodology, Writing - review & editing. **Peng Luo:** Formal analysis, Investigation, Writing - review & editing. **Yaoqiang Huang:** Formal analysis, Investigation, Writing - review & editing. **Ronghui Liang:** Formal analysis, Investigation, Writing - review & editing. **Kaiming Tang:** Formal analysis, Investigation, Writing - review & editing. **Zhenzhi Qin:** Formal analysis, Investigation, Writing - review & editing. **Chris Chun-Yiu Chan:** Formal analysis, Investigation, Writing - review & editing. **Kenn Ka-Heng Chik:** Formal analysis, Investigation, Writing - review & editing. **Jiang Du:** Formal analysis, Writing - review & editing. **Feifei Yin:** Funding acquisition, Supervision, Writing - review & editing. **Zi-Wei Ye:** Formal analysis, Writing - review & editing. **Hin Chu:** Formal analysis, Writing - review & editing. **Dong-Yan Jin:** Resources, Writing - review & editing. **Kwok-Yung Yuen:** Funding acquisition, Writing - review & editing. **Jasper Fuk-Woo Chan:** Conceptualization, Formal analysis, Funding acquisition, Project administration, Writing - original draft, Writing - review & editing. **Shuofeng Yuan:** Conceptualization, Formal analysis, Funding acquisition, Project administration, Writing - original draft, Writing - review & editing.

## Declaration of Competing Interest

The authors declare the following financial interests/personal relationships which may be considered as potential competing interests: J.F.-W.C. has received travel grants from Pfizer Corporation Hong Kong and Astellas Pharma Hong Kong Corporation Limited, and was an invited speaker for Gilead Sciences Hong Kong Limited and Luminex Corporation. The other authors declare no conflict of interests.

## Appendix A. Supplementary data

Supplementary data to this article can be found online at <https://doi.org/10.1016/j.csbj.2021.09.034>.

## References

- [1] Yu X-J, Liang M-F, Zhang S-Y, Liu Y, Li J-D, Sun Y-L, et al. Fever with thrombocytopenia associated with a novel bunyavirus in China. *N Engl J Med* 2011;364(16):1523–32.
- [2] Liu Q, He B, Huang S-Y, Wei F, Zhu X-Q. Severe fever with thrombocytopenia syndrome, an emerging tick-borne zoonosis. *Lancet Infect Dis* 2014;14(8):763–72.
- [3] Takahashi T et al. The first identification and retrospective study of Severe Fever with Thrombocytopenia Syndrome in Japan. *J Infect Dis* 2014;209(6):816–27.
- [4] Yoshikawa T, Shimojima M, Fukushi S, Tani H, Fukuma A, Taniguchi S, et al. Phylogenetic and Geographic Relationships of Severe Fever With Thrombocytopenia Syndrome Virus in China, South Korea, and Japan. *J Infect Dis* 2015;212(6):889–98.
- [5] Tran XC, Yun Y, Van An Le, Kim S-H, Thao NTP, Man PKC, et al. Endemic severe fever with thrombocytopenia syndrome vietnam. *Emerg Infect Dis* 2019;25(5):1029–31.
- [6] Liu W et al. Case-fatality ratio and effectiveness of ribavirin therapy among hospitalized patients in china who had severe fever with thrombocytopenia syndrome. *Clin Infect Dis* 2013;57(9):1292–9.
- [7] Liu S, Chai C, Wang C, Amer S, Lv H, He H, et al. Systematic review of severe fever with thrombocytopenia syndrome: virology, epidemiology, and clinical characteristics. *Rev Med Virol* 2014;24(2):90–102.
- [8] Yuan S et al. Viruses harness YxxO motif to interact with host AP2M1 for replication: A vulnerable broad-spectrum antiviral target. *Sci Adv* 2020;6(35).
- [9] Liu S, Liu H, Kang J, Xu L, Zhang K, Li X, et al. The severe fever with thrombocytopenia syndrome virus NSs protein interacts with CDK1 to induce G2 cell cycle arrest and positively regulate viral replication. *J Virol* 2020;94(6). <https://doi.org/10.1128/JVI.01575-19>.
- [10] Ning YJ et al. Viral suppression of innate immunity via spatial isolation of TBK1/IKKepsilon from mitochondrial antiviral platform. *J Mol Cell Biol* 2014;6(4):324–37.
- [11] Liu S, Liu H, Zhang K, Li X, Duan Y, Wang Z, et al. Proteasome inhibitor PS-341 effectively blocks infection by the severe fever with thrombocytopenia syndrome virus. *Virol Sin* 2019;34(5):572–82.
- [12] Yuan S, Chan J-W, Ye Z-W, Wen L, Tsang T-W, Cao J, et al. Screening of an FDA-approved drug library with a two-tier system identifies an entry inhibitor of severe fever with thrombocytopenia syndrome virus. *Viruses* 2019;11(4):385. <https://doi.org/10.3390/v11040385>.
- [13] Yuan S, Yin X, Meng X, Chan J-W, Ye Z-W, Riva L, et al. Clofazimine broadly inhibits coronaviruses including SARS-CoV-2. *Nature* 2021;593(7859):418–23.
- [14] Yuan S, Wang R, Chan J-W, Zhang AJ, Cheng T, Chik K-H, et al. Metallodrug ranitidine bismuth citrate suppresses SARS-CoV-2 replication and relieves virus-associated pneumonia in Syrian hamsters. *Nat Microbiol* 2020;5(11):1439–48.
- [15] Ahmad L et al. Novel N-substituted 5-phosphate-d-arabinonamide derivatives as strong inhibitors of phosphoglucose isomerases: synthesis, structure-activity relationship and crystallographic studies. *Bioorg Chem* 2020;102:104048.
- [16] Olsson MHM, Søndergaard CR, Rostkowski M, Jensen JH. PROPKA3: consistent treatment of internal and surface residues in empirical pKa predictions. *J Chem Theory Comput* 2011;7(2):525–37.
- [17] Stroganov OV, Novikov FN, Stroylov VS, Kulkov V, Chilov GG. Lead finder: an approach to improve accuracy of protein-ligand docking, binding energy estimation, and virtual screening. *J Chem Inf Model* 2008;48(12):2371–85.
- [18] Yu G, Wang L-G, Han Y, He Q-Y. clusterProfiler: an R package for comparing biological themes among gene clusters. *OMICS* 2012;16(5):284–7.
- [19] Law V, Knox C, Djoumbou Y, Jewison T, Guo AC, Liu Y, et al. DrugBank 4.0: shedding new light on drug metabolism. *Nucleic Acids Res* 2014;42(D1):D1091–7.
- [20] Lum KK, Cristea IM. Proteomic approaches to uncovering virus-host protein interactions during the progression of viral infection. *Expert Rev Proteomics* 2016;13(3):325–40.
- [21] Maude RJ, Woodrow CJ, White LJ. Artemisinin Antimalarials: Preserving the “Magic Bullet”. *Drug Dev Res* 2010;71(1):12–9.

- [22] Efferth T, Romero M, Wolf D, Stamminger T, Marin JG, Marschall M. The antiviral activities of artemisinin and artesunate. *Clin Infect Dis* 2008;47(6):804–11.
- [23] Nemunaitis J, Mita A, Stephenson J, Mita MM, Sarantopoulos J, Padmanabhanlyer S, et al. Pharmacokinetic study of omacetaxine mepesuccinate administered subcutaneously to patients with advanced solid and hematologic tumors. *Cancer Chemother Pharmacol* 2013;71(1):35–41.
- [24] Zhou H, Sun Y, Guo Yu, Lou Z. Structural perspective on the formation of ribonucleoprotein complex in negative-sense single-stranded RNA viruses. *Trends Microbiol* 2013;21(9):475–84.
- [25] Sun Y, Li J, Gao GF, Tien Po, Liu W. Bunyavirales ribonucleoproteins: the viral replication and transcription machinery. *Crit Rev Microbiol* 2018;44(5):522–40.
- [26] Jiao L, Ouyang S, Liang M, Niu F, Shaw N, Wu W, et al. Structure of severe fever with thrombocytopenia syndrome virus nucleocapsid protein in complex with suramin reveals therapeutic potential. *J Virol* 2013;87(12):6829–39.
- [27] Zhou H, Sun Y, Wang Y, Liu M, Liu C, Wang W, et al. The nucleoprotein of severe fever with thrombocytopenia syndrome virus processes a stable hexameric ring to facilitate RNA encapsidation. *Protein Cell* 2013;4(6):445–55.
- [28] McMullan LK, Folk SM, Kelly AJ, MacNeil A, Goldsmith CS, Metcalfe MG, et al. A new phlebovirus associated with severe febrile illness in Missouri. *N Engl J Med* 2012;367(9):834–41.
- [29] Shen S, Duan X, Wang Bo, Zhu L, Zhang Y, Zhang J, et al. A novel tick-borne phlebovirus, closely related to severe fever with thrombocytopenia syndrome virus and Heartland virus, is a potential pathogen. *Emerg Microbes Infect* 2018;7(1):1–14.